WORLD CONFERENCE ON TIMBER ENGINEERING 2025
BRISBANE, AUSTRALIA
Advancing Timber for the Future Built Environment

A study on the bending Behavior of Moment-Resisting Joints with LSB and GIR under High Axial Forces

Hwisu Kim[1], Atsuo Takino[2], Makoto Nakatani[3] , Takuro Mori[4] , Hiroki Ishiyama[5] , Seiji Mukaide[6]

ABSTRACT: In this paper, we focused on column-base joints used in mid- to high-rise wooden buildings, and conducted bending experiments under compressive axial force, to verify the fracture characteristics and mechanical properties. As test specimens, wooden moment-resisting joints with LSB and GIR are used. In the case where there was no axial force, brittle fracture occurred due to the LSB and GIR being pulled out, but as the axial force increased, nonlinearity was observed in the load deformation relationshi. When the wood underwent compressive failure, deformation continued to progress, even after the maximum load was reached, while the load decreased. Using the compressive strength of the wood and the tensile strength of the LSB and GIR, the N-M interaction off the yield strength was calculated and compared with the experimental results, and the corresponding results for the failure mode were obtained.

KEYWORDS: Wooden moment-resisting joint, Column-base joint, LSB, GIR, N-M Interaction

1 – INTRODUCTION

In Japan, since the revision of the Building Standards Acts in 2000, the development of fire-resistant wooden structural components has progressed. From around 2010 onward, the commercialization of such components has enabled the construction of wooden buildings in urban areas. As a result, medium- to large-scale general contractors and architectural design firms have begun to show interest in wooden structures in urban settings. Traditionally, wooden buildings have primarily been low-rise structures, and seismic design has mainly focused on shear force considerations. Consequently, significant efforts have been made to develop high-strength shear walls and moment-resisting joints. On the other hand, actual design cases of mid- to high-rise wooden buildings remain extremely limited. Only a few general contractors and design firms have been conducting experiments and advancing their designs. In reinforced concrete and steel structures, it is common practice to consider the N-M interaction during the design process. In column experiments, the shear force is typically applied while maintaining the axial force. However, in the field of timber structures, such experimental cases are rare, and naturally, the N-M interaction is seldom considered in the design process. Therefore, this study experimentally investigates the N-M interaction, which has been largely unexamined in timber structures. Specifically, bending tests were conducted on column-base joints under compressive axial force to examine their mechanical behavior. The study focused on LSB and GIR joints, which are expected to exhibit high strength and stiffness.

2 – EXPERIMENTAL METHOD

The list of test specimens is shown in Table 1. For all the test specimens, the glued laminated timber used was European red pine (pinus sylvestris/ E105-F300) with a width of 120 mm, a depth of 600 mm, and a length of 2,000mm. The LSB used had a total length of 460 mm, an effective thread length of 400 mm, a threaded section length of 40 mm, a minor diameter of 20 mm, and a major diameter of 25 mm. It was made of SNR490B steel. The GIR used had a total length of 580 mm and a diameter of 22 mm, and was made of a SD345 deformed reinforcing bar. In addition, epoxy resin adhesives were used for the GIR joint. The method of applying forces is shown in Fig.1, and the details of column-based joints are shown in Fig.2.

[1]Hwisu Kim, Graduate School of Engineering, Osaka Institute of Technology, Osaka, Japan, m1m24209@oit.ac.jp

[2]Atsuo Takino, Graduate School of Engineering, Osaka Institute of Technology, Osaka, Japan, atsuo.takino@oit.ac.jp

[3]Makoto Nakatani, Miyazaki Pref. Wood Utilization Research Center, Miyazaki, Japan, nakatani-makoto@pref.miyazaki.lg.jp

[4]Takuro Mori, Graduate School of Advanced Science and Engineering, Hiroshima University, Hiroshima, Japan, moritaku@hiroshima-u.ac.jp

[5]Hiroki Ishiyama, Graduate School of Engineering, Osaka Metropolitan University, Osaka, Japan, ishiyama@omu.ac.jp

[6]Seiji Mukaide, Graduate School of Engineering, Osaka Institute of Technology, Osaka, Japan, seiji.mukaide@oit.ac.jp

https://doi.org/10.52202/080513-0207

The column-based joints of the specimens were fixed to the steel jig. Horizontal and axial forces were applied using vertical and horizontal hydraulic jacks installed at the top. The LSB and GIR were connected to the steel jig using high tension bolts (LSB: M12/GIR: M27). In this study, we focused on joints made of LSB and GIR with wood, so steel joints with ductility were not used, but LSB and GIR were jointed directly to the steel jig.

The axial forces applied were 250 kN, 300kN, 500kN, 667kN and 1000 kN, corresponding to 0.15, 0.18, 0.3, 0.4 and 0.6 times the compressive strength of glued laminated timber (Fc = 23.2 N/mm²). We also tested a specimen with no axial force for comparison. The method of applying the load was displacement-controlled through drift angles, applying positive and negative alternating cyclic forces at drift angles of 1/450, 1/300, 1/200, 1/150, 1/100, 1/75 and 1/50 radians, with two repetitions at each dfift angle. After that, one-sided forces were applied until the specimen failed.

Table.1 The list of test specimen

Specimens	Joints	Axial forces
LSB-0	LSB	0kN
LSB-250		250kN
LSB-300		300kN
LSB-500		500kN
LSB-667		667kN
LSB-1000		1000kN
GIR-0	GIR	0kN
GIR-250		250kN
GIR-300		300kN
GIR-500		500kN
GIR-667		667kN
GIR-1000		1000kN

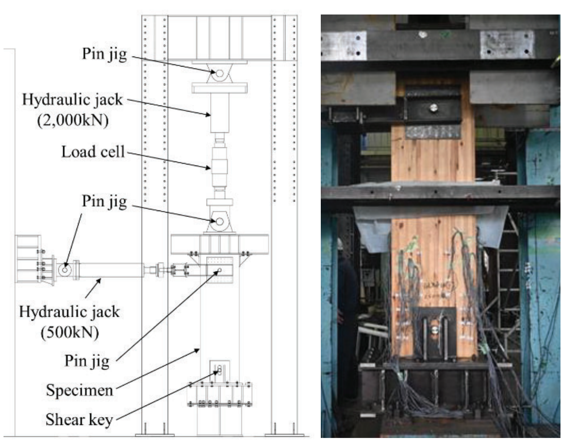

Fig.1 The method of applying forces

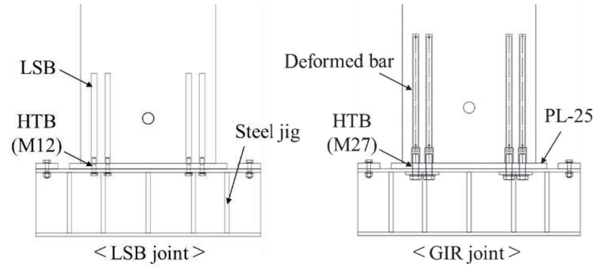

Fig.2 The details of column based-joints

3 – RESULTS

The load-drift angle relationships are shown in Fig.3. The list of yield strength *Py*, the drift angle at yield strength *Ry* and maximum strength *Pmax* of each specimen is shown in Table.2. The representative failure modes are shown in Fig.4 to 6. It should be noted that for the LSB-300, the load on the negative loading side could not be recorded due to an installation error in the load cell.

For the LSB specimens, In the case where there was no axial force, brittle fracture occurred due to the LSB being pulled out before 1/50rad. In the LSB-250 specimen, the tensile-side HTB ruptured immediately after exceeding 1/50rad, resulting in a sharp decrease in load. In the LSB-300 specimen, nonlinear behavior was observed beyond 1/50rad, followed by tensile-side HTB rupture. In the LSB-500 specimen, after exceeding 1/50 rad, the load began to stabilize, but subsequently, the tensile-side HTB ruptured. In the LSB-667 specimen, after exceeding 1/50 rad, the compression failure of wood and shear cracks were observed. When the load began to stabilize, LSB being pulle out, leading to a gradual load decrease. In the LSB-1000 specimen, the load decreased due to compression failure of the wood and progressed until the end of the test. Regarding HTB ruptures, high-strength HTB with a strength grade of 12.9 were used to prevent HTB rupture before LSB being pulled out. However, compared to standard joints, the steel plates of the experimental fixture were thicker, and HTBs with a long screw were used. As a result, bending moments acted on the threaded ends, which is considered to be the cause of HTB rupture.

For the GIR specimens, In the case where there was no axial force, splitting failure of tensile- side wood at the GIR joints occurred immediately after exceeding 1/50rad, resulting in a sharp decrease in load. As the axial force increased, the compression failure of the wood became more pronounced, and nonlinear behavior gradually developed, similar to the LSB specimens. In the GIR-250, GIR-300, and GIR-500 specimens, splitting failure of tensile-side wood occurred immediately after exceeding 1/50rad, resulting in a sharp decrease in load. In the GIR-

https://doi.org/10.52202/080513-0207

667 specimen, the compression failure of wood was observed beyond 1/50rad, but ultimately, a sudden load decrease occurred around 1/30rad due to splitting failure of tensile-side wood. In GIR-1000 specimen, shear failure extended throughout the laminated timber, resulting in a sharp decrease in load.

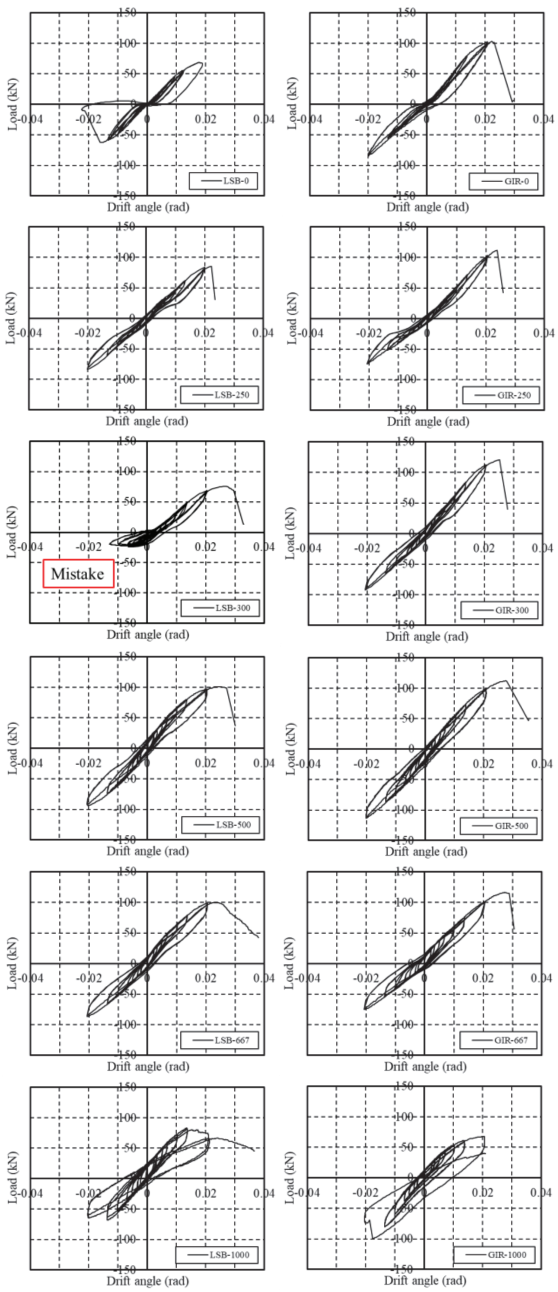

Fig.3 The load- drift angle relationship

Table.2 The list of various strength of each specimen

Specimens	Py[kN]	Ry[rad]	Pmax[kN]
LSB-0	47.8	0.01	68.36
LSB-250	41.7	0.009	85.4
LSB-300	58.7	0.016	75.9
LSB-500	54.2	0.007	100.8
LSB-667	49.8	0.008	99.7
LSB-1000	40.5	0.003	82.8
GIR-0	86.3	0.015	102.7
GIR-250	80.8	0.015	111.5
GIR-300	79.3	0.013	120.8
GIR-500	60.5	0.011	111.3
GIR-667	58.9	0.010	116.4
GIR-1000	38.6	0.005	67.7

〈LSB-300〉

〈LSB-667〉

Fig.4 The HTB fracture and LSB pullout failure

〈LSB-667〉

〈GIR-1000〉

Fig.5 The shear failure

〈GIR-250〉

〈LSB-1000〉

Fig.6 The splitting failure and compression failure

https://doi.org/10.52202/080513-0207

The strain distribution diagram for each drift angle in the LSB and GIR specimens are shown in Fig.7. They were measured at a height of 100 mm from the end grain (tensile strain is taken as positive.)

As the axial forces increase, the compressive strain on the tensile side of the wood also increases. However, as the drift angle becomes larger, the compressive strain on the tensile side of the wood tends to become negligible.

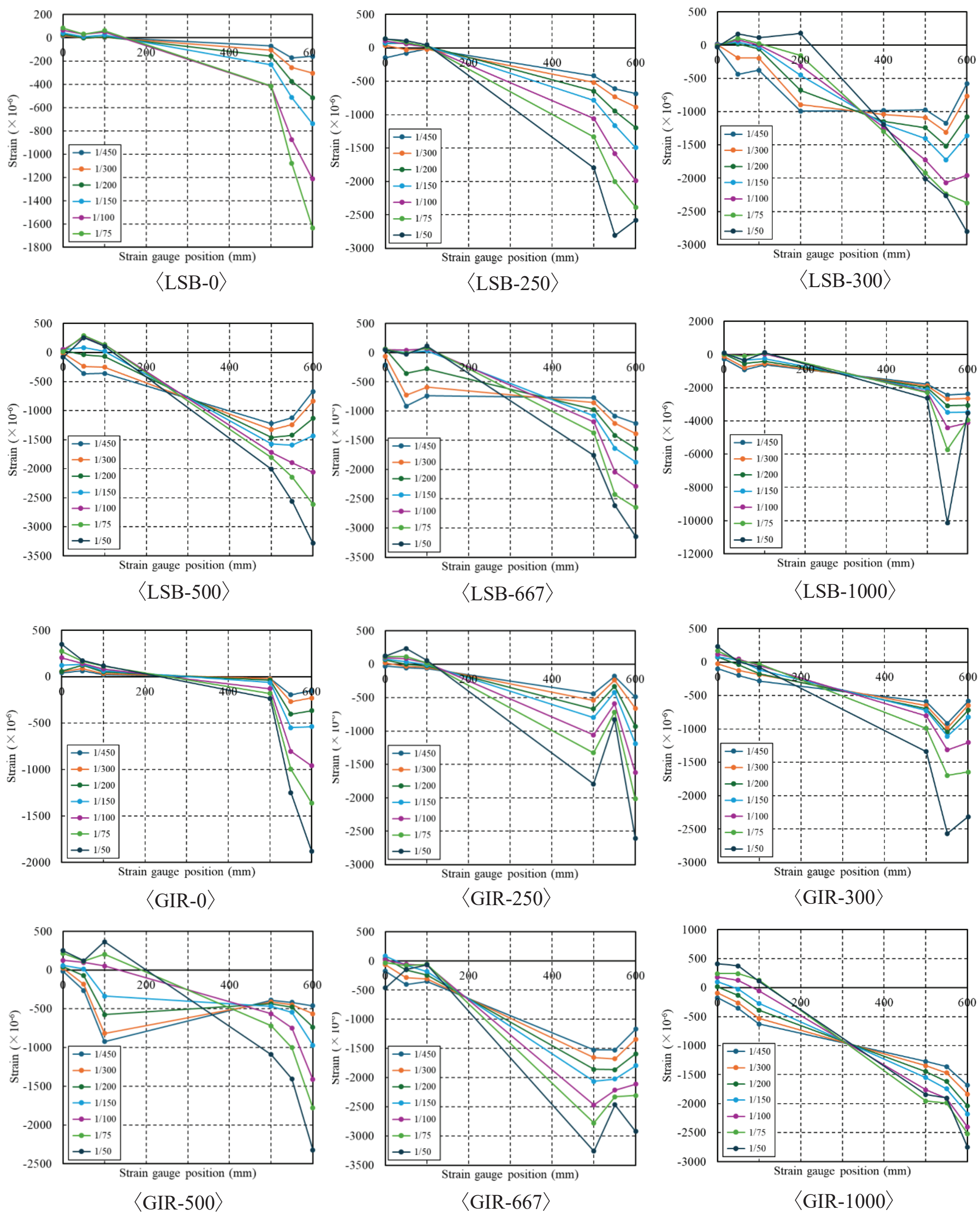

Fig.7 The strain distribution diagrams for each drift angle

https://doi.org/10.52202/080513-0207

4 – N-M interaction

Using the compressive strength of the wood and the tensile strength of the LSB, the N-M interaction of LSB specimen at the yield strength was calculated. Considering the equilibrium of force with Navier's hypothesis at the end grain , the following four states were considered, (i) Wood bears only compressive forces (wood yields in compression), (ii) Wood bears compressive forces and LSB bears tensile forces respectively (wood yields in compression), (iii) Wood bears compressive forces and LSB bears tensile forces respectively (LSB yields in tension), (iv) LSB bears tensile forces only (LSB yields in tension). (Fig.8).

For the calculation of the compressive yield load of the wood, the compressive design strength of laminated timber, Fc=23.2 N/mm², was used. The loss of cross-sectional area due to the LSB and the contribution of the LSB to the compressive forces were not considered. The bearing stiffness of the compressive side of the wood was determined using the Young's modulus of laminated timber (E=10.5 kN/mm²), assuming an effective load-bearing length of 300 mm, yielding a bearing stiffness of 35 N/mm^3. For the calculation of the tensile yield load of the LSB, a tensile element experiment was conducted on an LSB specimen (Fig. 9), and the obtained results (Py =63.5 kN, δy=0.379 mm per LSB) were adopted. Although two LSBs were placed at each end, they were treated as a single unit for calculation purposes.

The N–M interaction (where compressive axial force is positive) is shown in Fig.10. The solid lines indicate the valid range of calculations under the given conditions. The experimental yield load Py was determined using a perfectly elastic-plastic approximation of the positive-side envelope curve, of the corresponding axial force that was obtained (Table 2). Additionally, the bending moment at the column base was determined, considering the additional moment caused by horizontal displacement of the vertical hydraulic jack. The distance for multiplying the horizontal load was taken as 1,750 mm, from the center of the horizontal jack to the end grain of the laminated timber.

Furthermore, the results at the maximum load are included in the figure for reference. Although some discrepancies were observed, the experimental results generally captured the calculated N–M interaction. However, the results for N=0 kN showed a larger error compared to other cases.

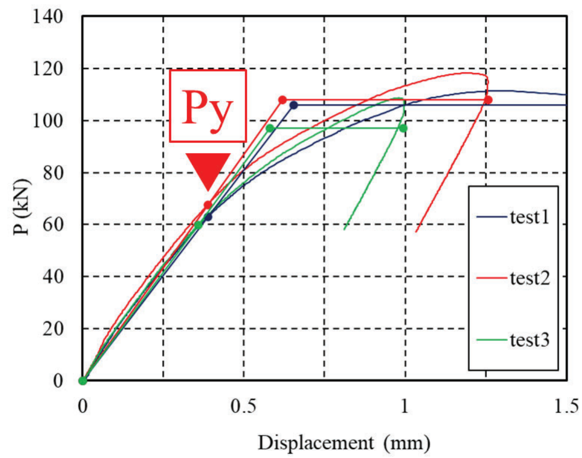

Fig.9 Tensile element experiment of the LSB

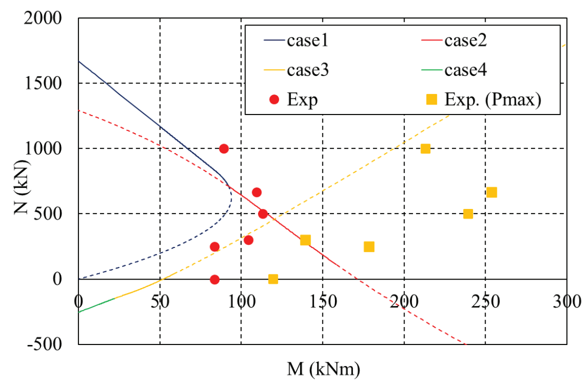

Fig.10 N-M interaction

Fig.12 Crushing of wood at end grain

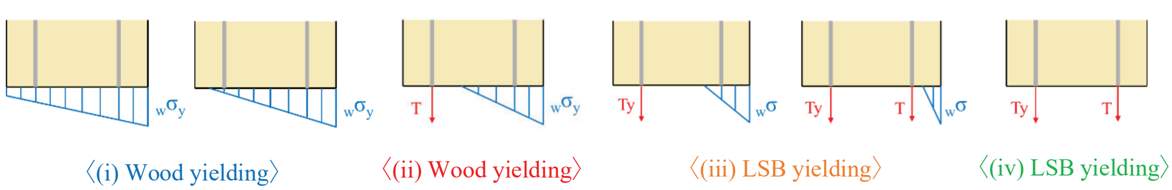

Fig.8 Classification of Stress States

https://doi.org/10.52202/080513-0207

5 – Comparison of strain distribution

The strain distribution at yield in the LSB specimen and the assumed failure characteristics based on the N-M interaction are compared in Fig. 11. Strain measurements were taken at the locations marked by circles in the figure, with the data points connected by straight lines. Additionally, the strain distributions corresponding to the axial forces during the experiment were plotted based on the N-M interaction. For the strain distribution determined by the compressive yield of the wood, the yield strain was assumed to be 2,210 μ, calculated from Fc = 23.2 N/mm² and E =10.5 kN/mm². For the strain distribution determined by the yield of the LSB, the compressive displacement of the wood was calculated under the assumption of plane restraint, and this value was divided by L = 300 mm to obtain the compressive strain of the wood.

The N=0 kN and 250 kN test results showed that the experimental strain distribution had a steeper gradient than the calculated one. As axial force increased, the experimental strain approached the assumed distribution with a more moderate gradient. The experiment confirmed that wood crushed at the end grain before buckling occurred(Fig.12). Since the calculation assumes bilinear bearing stiffness, the bearing stiffness may have changed between the initial loading phase and the compressive yield. At N=0 kN, the experimental My was 83.7 kNm, and the back-calculated LSB yield load was 164.1 kN, higher than the element test yield load of 63.5 kN. Fig.9 indicates that the yield load of the LSB was evaluated conservatively. While an estimate of approximately 80 kN is possible, the wood was assumed to be rigid in the calculations, suggesting that the actual bearing stiffness may be greater than the assumed kw=35 N/mm³. However, in this experiment, ductile elements commonly used in joints (typically incorporating a steel-based ductility mechanism) were not employed, meaning that the overall behavior was governed by the pull-out resistance of the LSB on the tensile side. As shown in Fig. 9, the LSB has almost no deformation capacity, resulting in very small displacement at yield. This suggests that the results may be significantly influenced by the assumptions made in the calculations for the N-M interaction.

6 – CONCLUSIONS AND RECOMMENDATIONS

In this paper, we conducted bending experiments under compressive an axial force, and verified the fracture characteristics and mechanical properties. The N-M interaction at yield is calculated for the LSB specimens and compared with the experimental results. In the future, it will be necessary to expand to the N-M interactions at the ultimate strength.

7 – ACKNOWLEDGEMENT

This research was funded by JSPS Grants-in-Aid for Scientific Research JP21H01478. I would like to express my gratitude to them.

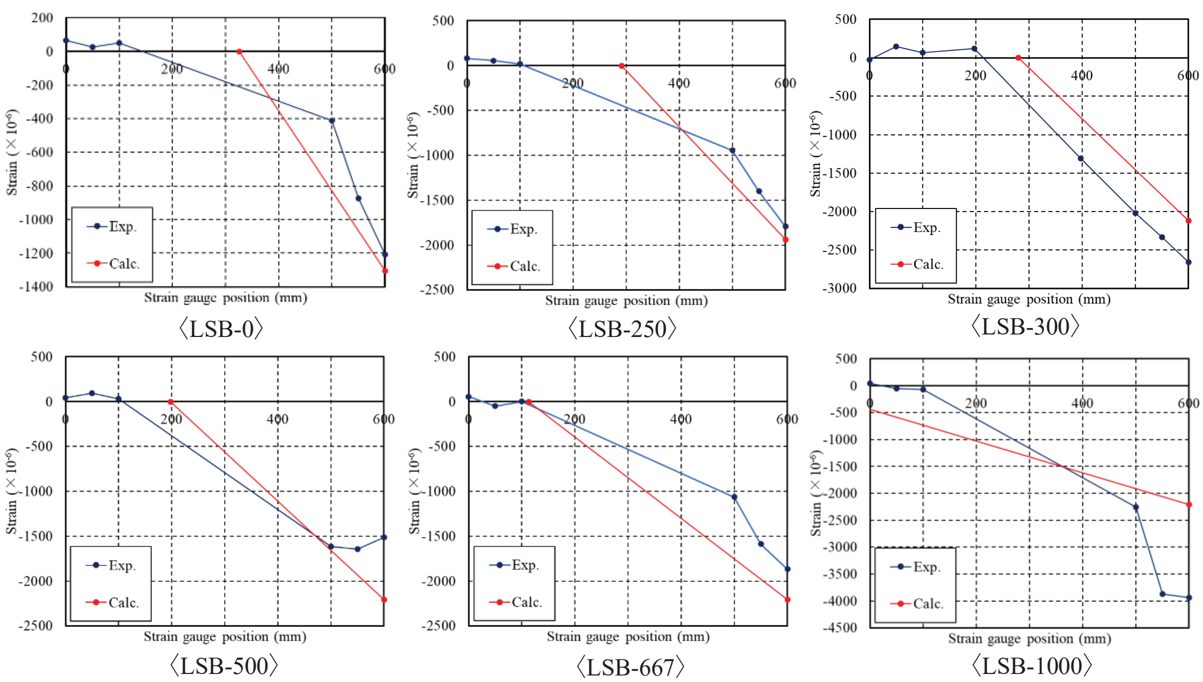

Fig.11 The comparison of strain distribution at yield and the assumed failure characteristics on the N-M interaction